JOURNAL OF MATERIALS SCIENCE 27 (1992) 1121–1128

Investigation of the displacement reaction in mixed AlN + TiO_2 powders

Part I *Microstructural changes at 1 atm N_2*

T. SPERISEN*, A. MOCELLIN*‡
* *Laboratoire de Céramique, Ecole Polytechnique Fédérale, Lausanne, Switzerland*
‡ *LSG2M–URA 159, Ecole des Mines, Nancy, France*

Micrometre-size AlN + TiO_2 powders in the molar ratio 2/1.5 were mixed, cold-pressed and heat-treated to 1400–1800 K in an AlN + N_2 = 1 atm buffer environment. Coarse AlN particles in fine TiO_2 powder, and TiO_2 single-crystal chips in fine AlN powder were also processed similarly. From X-ray diffraction and direct microstructural observations it is described and discussed that to a first approximation the overall reaction proceeds in three major steps: (i) reduction of TiO_2 to Ti_4O_7 or Ti_3O_5 with concurrent Al_2O_3 dissolution, (ii) formation of $Al_xTi_yO_5$ phases of either monoclinic or orthorhombic structure depending chiefly on the initial TiO_2 particle size, (iii) decomposition of such mixed oxide into Al_2O_3 + TiN. Simultaneously with these steps, the progressive oxidation of AlN to Al_2O_3 takes place at a rate which does not limit the overall reaction kinetics. Evidence is also provided that the reaction takes place in part via the transport of gaseous Al- and Ti-containing species, which calls for further investigation to be reported in the companion paper.

1. Introduction

Among a variety of procedures for producing ceramic–ceramic composites, displacement-reaction sintering or hot-pressing so far seems to have received but little attention. It basically consists of reacting a mixture of two compounds, e.g. AB + CD to yield the new combination AD + CB. Somewhat more complex reaction schemes may also be encountered as will be shown in this and the following paper which, rigorously speaking, may not always be referred to as "displacement reactions". But in practice an essential feature of such a family of chemical transformations, when taking place in solids, is to deliver two crystal lattices different from the starting ones. When working with powders, therefore, the resulting microstructures may display novel characteristics which are (for instance) more refined or more anisotropic. It is also conceivable that solid–solid interfaces be of different structures and compositions and that initial residual impurities be somehow redistributed. Finally, it seems worth mentioning that a wide range of possibilities also exists to prepare materials in which a reinforcing phase, either fibrous or not, would be bonded by such a chemically reacted matrix. A particular example would consist of using one of the product phases of the matrix as an inert filler to have some control over the final relative phase contents and detailed distributions of sizes and shapes.

Simple displacement reactions are well known to take place in oxide metal systems [1–3] and sulphide metal systems [4–6]. Double displacement reactions have also been reported in oxide–carbide [7], oxide–oxide [8, 9] and oxide–nitride [10, 11] combinations. But for the latter cases at least, very little is known so far about the corresponding detailed reaction mechanisms and microstructure changes, which precludes their potential for practical utilization in producing materials from being correctly assessed. Thus, focusing our attention to the special case of Al_2O_3–TiN particulate composites possibly useful as cutting tool or wear-resisting materials, we have undertaken to investigate some of the above-mentioned topics starting with AlN + TiO_2 powder mixtures. In previous work [12] some compositions in that system were explored and it was pointed out that an AlN to TiO_2 ratio of 2:1.5 yields formation of Al_2O_3 and TiN with a respective ratio 1:1.5 together with some 0.25 N_2 outgassing. Attention was therefore paid to that particular composition from the point of view of powder processing [13, 14] and preliminary mechanical characterization of the reacted hot-pressed Al_2O_3–1.5TiN particulate composite [13, 15]. Although no systematic study of the reaction mechanism has been published, an intermediate transient phase of the pseudo-brookite type was sometimes found to persist in the densified samples [12, 13], the influence of which was not evaluated. The reaction will be studied in greater detail with regard to the evolution of the nature and arrangement of solid phases and to the overall N_2 gas exchange within or out of the reacting medium. For that purpose the starting molar composition of the reacting mixture was set to 1.5TiO_2 + 2AlN which is known [12] to yield complete transformaton into Al_2O_3 + TiN.

0022–2461

In a companion paper [16] effects associated with the externally applied gas pressure, the gas phase composition within the porous samples and vapour transport contributions to the overall reaction will be investigated in greater detail. It will also be pointed out that changing the initial AlN to TiO_2 ratio within reasonable limits does not markedly affect the reaction mechanism. It should be kept in mind finally that sintering or conditions for densification are not to be considered in either this or the companion paper.

2. Experimental procedure

Three types of $1.5TiO_2 + 2AlN$ powder mixtures have been investigated, the initial characteristics of which are reported in Fig. 1 and Table I. The first mixture (hereafter referred to as FF) consists of both fine TiO_2 and AlN starting powders. The other two (labelled CC and CF) are prepared from both coarse TiO_2 and AlN, and coarse TiO_2 and fine AlN, respectively. All mixtures were ball-milled in isopropyl alcohol, and then spray-dried [13, 14]. Pellets 10 mm in diameter by 10–15 mm high were uniaxially pressed to 200 MPa in a steel die, then placed in Al_2O_3 crucibles and covered with their corresponding AlN powder as buffer. Heat treatments were carried out in an Al_2O_3 tube furnace in the temperature range 1400–1800 K under flowing N_2 containing 1 v.p.m. O_2 according to the supplier.

After cooling under nitrogen at 200 K min^{-1}, the reacted samples were cut into two parts. The first was embedded in resin under vacuum and diamond-polished for microstructural evaluation, i.e. optical and scanning electron microscopy and electron-probe microanalysis (EPMA). A thin carbon layer was vacuum-deposited on such samples when necessary. The second part was crushed back into powder for X-ray diffraction analyses using CuK_α radiation with a Siemens D-500 diffractometer. For lattice parameter evaluations photon counts were recorded stepwise at angle positions 0.02° apart for 8–10 s, thus yielding accuracies better than 10^{-3} on d-spacings when the corresponding 2θ values were in excess of 30°. Consequently, uncertainty limits on the lattice parameter values to be reported below are those that arise from a least-squares fit on indexing the diffraction pattern, based on a number of reflections which exceeds five times the number of variables for a given lattice (i.e. ~ 22 lines for an orthorhombic structure).

A variety of complementary experiments were also performed to help clarify issues or check interpretations. These will be described in greater detail during the course of discussion, but typically included spray-dried Al_2O_3–TiO_2 mixtures heat-treated under reducing conditions, large TiO_2 single crystals (> 100 μm) embedded in excess AlN powder compared to the standard $1.5TiO_2/2AlN$ ratio. It is also worth quoting some runs of high-temperature neutron diffraction ($\lambda = 0.252$ nm from a graphite monochromator, neutron flux = 1.6×10^6 cm^{-2} s^{-1}, carried out at Institut Laue–Langevin, Grenoble) on cold-isostatically-pressed cylinders (10 mm diameter by ~ 120 mm long) suspended across the neutron beam in a vacuum furnace with Nb thermoelements. The neutron diffraction experiments used a curved multidetector (5 cells per degree 2θ) in the 40–117° 2θ range; FWHM resolution was 0.2 at $2\theta = 40°$ and 0.8 at $2\theta = 115°$.

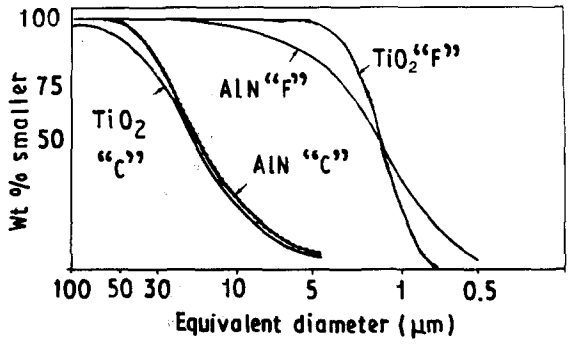

Figure 1 Particle size distributions of initial AlN and TiO_2 powders.

3. Results and discussion

In all the investigated samples, X-ray diffraction analyses show that the starting AlN phase gradually disappears during high-temperature treatment and α-Al_2O_3 lines are detected rather early and subsequently intensify, but not in quantitative relation with the corresponding AlN intensity decrease. Changes affecting the initial TiO_2 phase are much more

TABLE I Cemical analyses of initial powders (from suppliers)

Powder[a]	Composition (wt %)									
	Al	O	C	Fe	Ti	Si	S	Sn	Mg, Ca Na, K	Others
AlN "F" (1)	> 64	2.1	0.06	7×10^{-3}	–	–	–	–	–	$< 10^{-2}$
AlN "C" (2)	–	–	–	–	–	–	–	–	–	< 1
TiO_2 "F" (3)	$< 2 \times 10^{-3}$	–	–	$< 10^{-2}$	60	$< 10^{-2}$	$< 10^{-2}$	$< 3 \times 10^{-3}$	$< 4 \times 10^{-2}$	$< 2 \times 10^{-2}$
TiO_2 "C" (4)	10^{-3}	–	–	10^{-3}	60	5×10^{-3}	10^{-2}	5×10^{-3}	4×10^{-3}	$< 10^{-2}$

[a](1) H.C. Starck grade C; (2) Ventron; (3) Tioxide H.P.; (4) Tioxide, lot 1708.

complex and appear to proceed in three major steps, as already pointed out [12]. First, the rutile diffraction lines quickly disappear while a complex pattern corresponding to combinations of Magneli phases Ti_nO_{2n-1} builds up (together with some Al_2O_3 being formed). Secondly, when the Magneli index n has been sufficiently decreased, Ti_3O_5-based solid solutions, sometimes but not always with a pseudo-brookite crystal structure, begin to form by incorporating some Al_2O_3 as shown by direct EPMA evidence. Almost simultaneously, the TiN diffraction lines begin to show up. Thirdly, after going through a maximum the Ti_3O_5 solid-solution content then decreases, sometimes until complete disappearance, whereas the Al_2O_3 and TiN intensities increase toward their final levels in the fully reacted samples, it being kept in mind that residual AlN is detectable until rather late in the process. The general scenario thus outlined is supported and illustrated by the evidence of Figs 2 and 3. It develops roughly independently of the initial AlN particle size as far as can be judged from X-ray diffraction and microstructure observation. The use of coarse powders therefore provides a microstructure upscaling which facilitates observations.

However, varying the initial TiO_2 particle size has an effect on the kinetics, which will be discussed further. Discussion will now focus on the solid-phase evolution taking place in this general three-step reaction, and will make use of thermochemical arguments to confirm the reaction path at constant external $p_{N_2} = 1$ atm and under the simplifying assumption of constant bulk density. In fact, specific gravity measurements on samples before the onset of the reaction and after its completion yield relative values of $\sim 52\%$ and 45% respectively, which accounting for a relative molar volume change $\Delta V/V \approx 20\%$ corresponds to a maximum net densification of about 4%, irrespective of the type of powder mixture being investigated. Such a densification in the present operating conditions is thought not to have affected the progress of chemical reactions, since it corresponds roughly to a 1.5% linear shrinkage and thus a rather limited change of overall permeability of the samples.

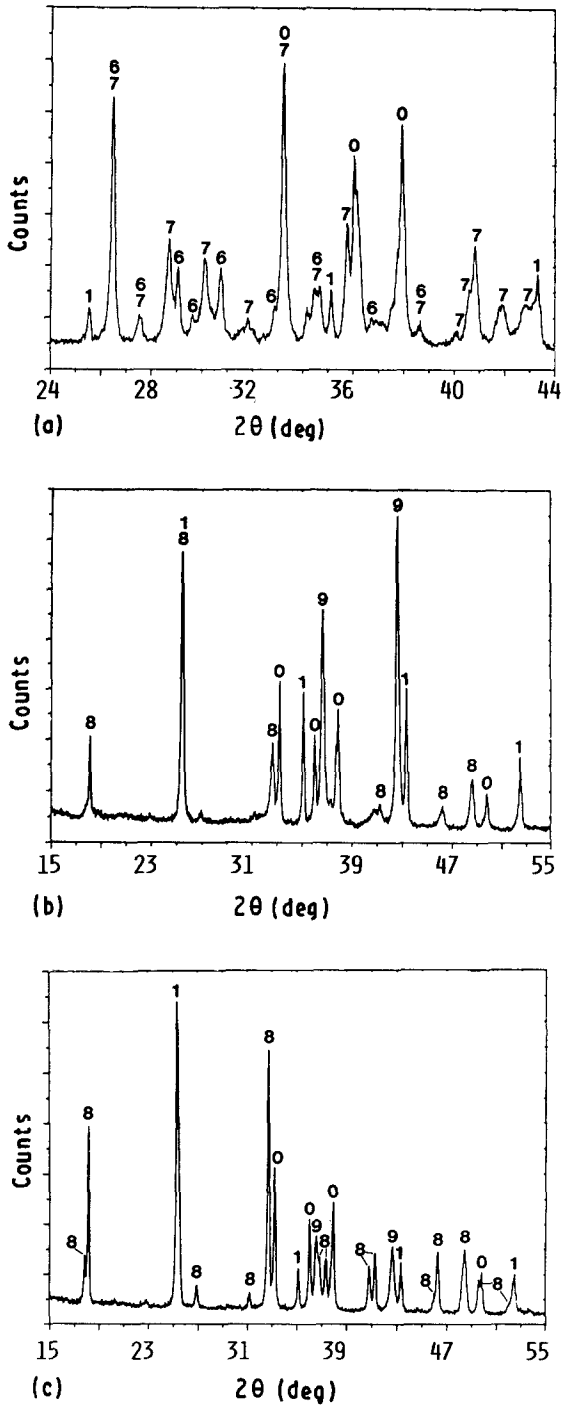

Figure 2 Typical X-ray diffraction patterns during reaction of fine $\frac{3}{2}TiO_2 + 2AlN$ powder mixtures at 1500 K: (a) initial step (after 5 min), (b) intermediate step (after 15 min), (c) final step (after 45 min). Line identification: (0) AlN, (1) Al_2O_3, (6) Ti_5O_9, (7) Ti_6O_{11}, (8) $Al_xTi_yO_5$, (9) TiN.

3.1. Initial reaction step: reduction of rutile

The progressive reduction of the starting TiO_2 particles to Magneli-type phases Ti_nO_{2n-1} as the initial reaction step is demonstrated by X-ray diffraction (Fig. 2a) and may be observed directly through optical microscopy in samples containing large TiO_2 particles (Fig. 3a and b). It therefore appears that oxygen liberated by the reduction of TiO_2 is immediately taken up to oxidize AlN, so that at least partial dissolution of Al_2O_3 into Ti_nO_{2n-1} readily takes place as it is known to do in TiO_2 [17], and could indeed be detected by EPMA. However, no nitrogen was detected by EPMA in the Magneli-type solid solutions, suggesting that this species is liberated to the gas phase. Slight local increases of p_{N_2} above the externally applied 1 atm must therefore result. The kinetics of Al dissolution into Ti_nO_{2n-1} has not been further investigated.

On the other hand, it was also found that, everything else being equal, the most reduced of the detectable Ti_nO_{2n-1} phases, i.e. that with the smallest n value, was dependent on the initial TiO_2 particle size. With fine powders, Ti_4O_7 is the last one to be observed before a new phase of composition $Al_xTi_yO_5$ is formed [18]. In coarse particles, however, Ti_3O_5 patches are formed in outer zones (Fig. 3a and b) and are easily recognized as containing a microcrack network, presumably formed during cooling through ~ 400 K, the α- to β-Ti_3O_5 phase transformation temperature. The reason for such differences is

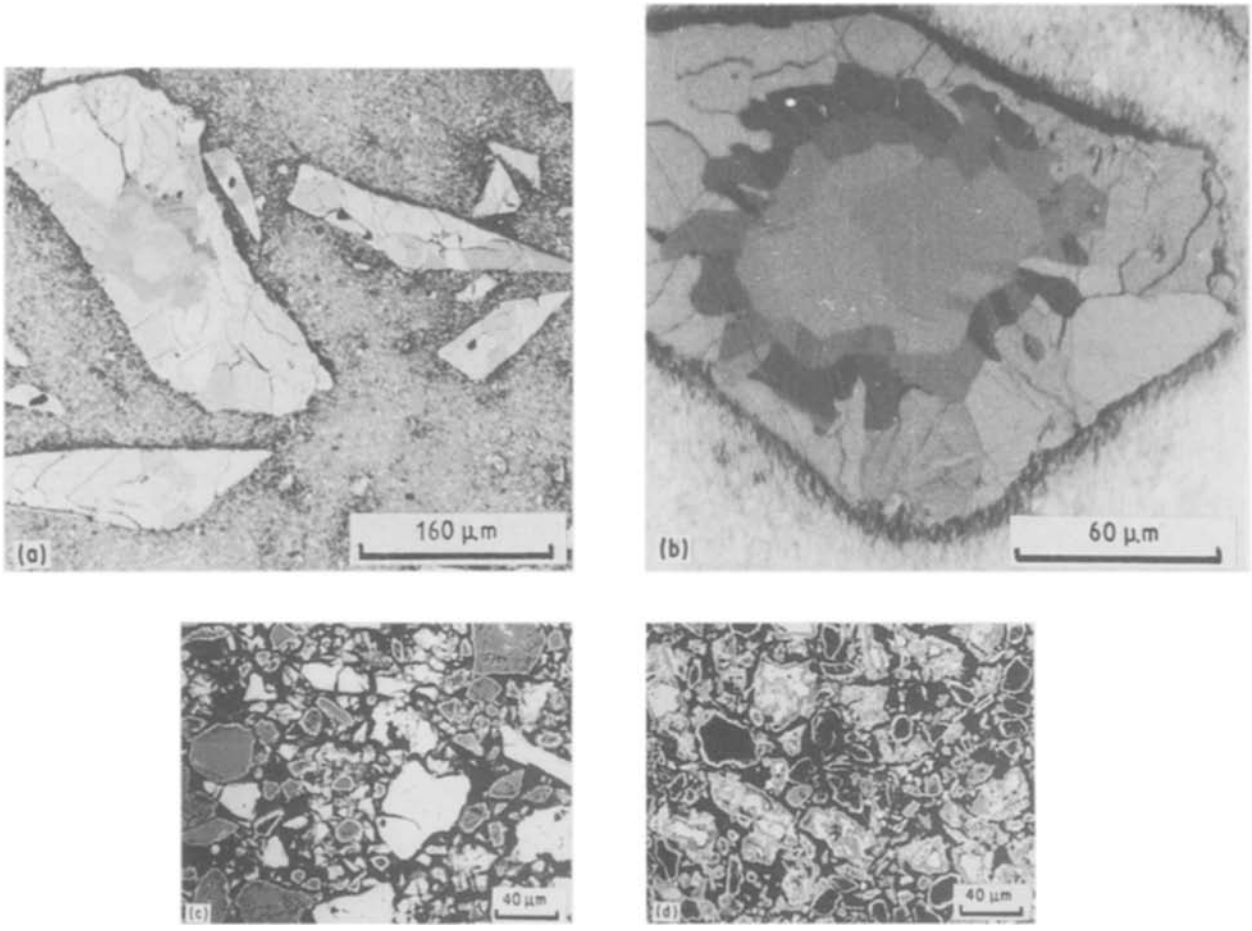

Figure 3 Characteristic microstructures of AlN + TiO_2 particle mixtures at successive reactions stages. (a. b) Initial step: partially reduced TiO_2 chips in AlN matrix (contrast variations correspond to different Magneli phases). (c) Intermediate step: formation of $Al_xTi_yO_5$ mixed oxide and primary TiN layers on AlN particles. (d) Final step: decomposition of Al–Ti mixed oxide into TiN + Al_2O_3 and continuing AlN oxidation. Al phases dark and Ti phases clear on micrographs (c) and (d).

thought to be related to the total amount of Al_2O_3 that can be dissolved during the given reaction time. Fine particles saturate faster than coarse ones and subsequently give rise to different crystalline phases, depending upon their Al content and the oxygen partial pressure in their vicinity which also are both related [18].

The preceding discussion may be summarized into the following system of coupled chemical reactions in which stoichiometric coefficients have been adjusted to correspond to the initial mixture composition:

$$\frac{3}{2}TiO_2 \rightarrow \frac{3}{8}Ti_4O_7 + \frac{3}{16}O_2 \quad (1)$$

$$2AlN + \frac{3}{16}O_2 \rightarrow \frac{7}{4}AlN + \frac{1}{8}Al_2O_3 + \frac{1}{8}N_2 \quad (2)$$

If it is now assumed that the oxygen partial pressure at the reaction sites is not inferior to that set by the AlN–Al_2O_3 equilibrium for $p_{N_2} \approx 1$ atm, then thermochemical calculations of the stability ranges for Ti suboxides using available data [19] show (Fig. 4) that TiO_2 can in principle be reduced to Ti_2O_3. The fact that Ti_3O_5 or Ti_3O_5-based solutions containing Al are observed after reduction has proceeded down to

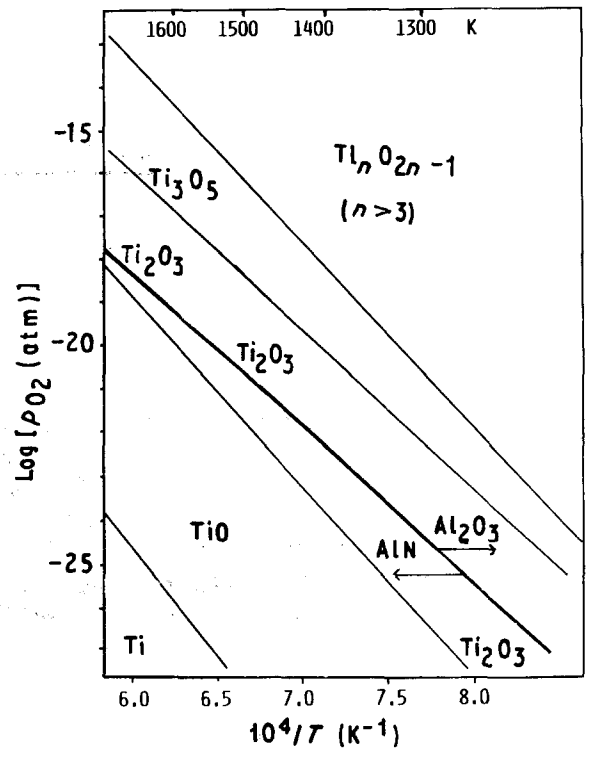

Figure 4 Calculated equilibrium solid-phase diagram of the Ti–O system under 1 atm N_2 pressure.

a p_{O_2} value which thus locates within the Ti_3O_5 stability field (Fig. 4) suggests that AlN oxidation is not rate-limiting at this stage. In the companion paper [16] a further discussion of the atmosphere-related mechanisms will be presented to support such a conclusion.

3.2. Intermediate reaction step: onset of TiN formation

The second major step of the reaction is somewhat more complex due to the variety of phases and compositions that Ti_4O_7 or Ti_3O_5 can yield on Al_2O_3 dissolution, and to the first production of TiN. Figs 2b and 5 show typical examples of post-cooling X-ray diffraction and high-temperature neutron diffraction spectra, respectively. The latter, where the time variation of intensities exceeding some level above background has been recorded, show the direct transformation of Ti_4O_7 into $Al_xTi_yO_5$-type phase with no intermediate Ti_3O_5 or Ti_3O_5 solution for the case of fine powder FF mixtures. Also visible in Fig. 5 is the beginning soon thereafter of some TiN diffraction. Such TiN is also noticeable in Fig. 2 showing the state of affairs in some FF mixtures after reaction has proceded further.

Rather different appears to be the behaviour of samples made from coarse TiO_2 powders and in which Ti_3O_5 lines are clearly seen as already mentioned. Fig. 6 shows that both the α and β modifications of Ti_3O_5 may at times be present even after prolonged heating at high temperatures. Since (Fig. 4) the oxidation of AlN would tend to reduce TiO_2 down to Ti_2O_3 and Al_2O_3 can dissolve in Ti suboxides, when the stage of Ti_4O_7 is reached, two alternative routes become possible.

On the one hand, Ti_4O_7 is further reduced to α-Ti_3O_5 which transforms into β-Ti_3O_5 after quenching when the Al_2O_3 content is very low. Formation of α-Ti_3O_5-based solutions in that case involves a reaction between Ti_3O_5 and Al_2O_3 such as that described elsewhere [18].

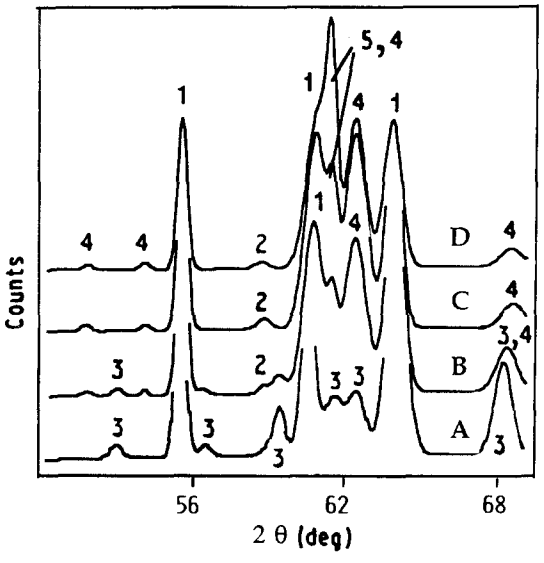

Figure 5 Neutron diffraction spectra recorded during the reaction of FF powder mixture at 1450 K (reaction time increases from A to D). Line identification (1) AlN, (2) Al_2O_3, (3) Ti_2O_3, (4) $Al_xTi_yO_5$, (5) TiN.

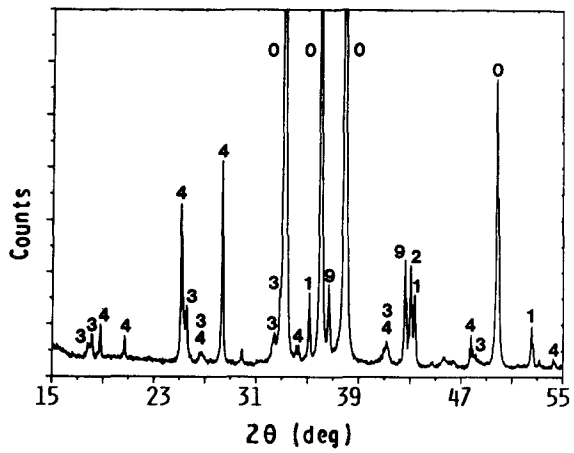

Figure 6 X-ray diffraction spectrum of partially reacted CF-type TiO_2–AlN mixture, showing that both α and β modifications of Ti_3O_5 may be present simultaneously. Line identification: (0) AlN, (1) Al_2O_3, (3) α-Ti_3O_5, (4) β-Ti_3O_5, (9) TiN.

On the other hand, Ti_4O_7 is reduced to an α-Ti_3O_5-based solution which retains its structure when cooling to room temperature to form monoclinic or even orthorhombic $Al_xTi_yO_5$ phases depending on whether the Al_2O_3 content of Ti_4O_7 was sufficiently high [18]. Deciding which route the system will follow therefore depends on the relative fluxes of aluminium into and of oxygen out of Ti_4O_7, which are both provided and consumed by nearby AlN, respectively.

In fine AlN–TiO_2 FF mixtures the $Al_xTi_yO_5$ phase can be indexed as an orthorhombic CmCm structure, the lattice parameters of which ($a_0 = 0.9745(5)$ nm, $b_0 = 0.7750(5)$ nm, $c_0 = 0.9916(4)$ nm) do not evolve once this phase is detected. Evaluation of x from X-ray diffraction can be done by comparison with literature data [18]. So a value of $x \approx 0.55$ could be estimated. If one assumes for simplicity that all the Al_2O_3 produced by step 1 (Equations 1 and 2) is dissolved into Ti_4O_7, the reduction of Al-saturated Ti_4O_7 will give $x = 0.42$ which is considered to be a limiting value for orthorhombic CmCm stability [20]. In coarse particles, on the other hand, a significant Al concentration gradient is established (Fig. 7) and only an outer shell of the particles is converted into pseudo-brookite whereas

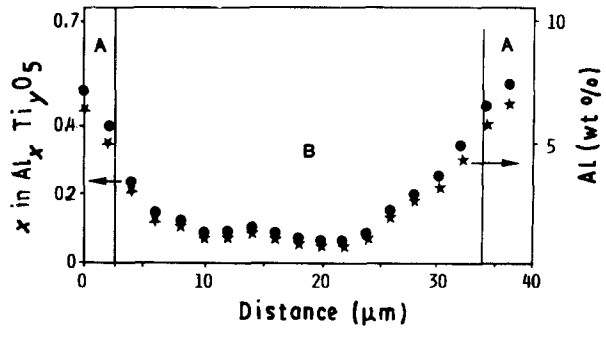

Figure 7 (*) Measured weight concentration of Al in large initial TiO_2 particle and (●) corresponding x estimates of $Al_xTi_yO_5$ composition. A and B refer to orthorhombic and monoclinic regions, respectively. 1 h at 1600 K in 1 atm N_2.

their cores remain monoclinic Ti_3O_5 solutions. EPMA (Fig. 7) in conjunction with micrographic evidence thus suggests that Al_2O_3 concentrations of about 0.3 and 5 wt % (giving respectively $x = 2 \times 10^{-2}$ and $x = 0.40$–0.45) are necessary to stabilize the α-Ti_3O_5 phase down to room temperature and yield the orthorhombic titanate, respectively. The latter estimation is in agreement with literature data [20] and with X-ray diffraction results.

Returning to the matter of first TiN formation, the peculiar growth habit as thin layers on AlN particles (Fig. 3c) suggests that it was built up via some vapour transport mechanism rather than by solid-state diffusion [16]. It is worth checking the thermodynamic feasibility of TiN formation from the stage the reacting system has reached. Fig. 8 shows the calculated phase diagram at 1600 K for the general system

$$Ti_nO_{2n-1} + \frac{n}{2}N_2 = nTiN + \left(\frac{2n-1}{2}\right)O_2 \quad (3)$$

with

$$\log p_{O_2} = \frac{2}{2n-1}\log K_n + \frac{n}{2n-1}\log p_{N_2} \quad (4)$$

where $\ln K_n = -\Delta G_n^\circ/RT$ and ΔG_n° is the Gibbs free energy change associated with Reaction 3.

It can be seen from such figures that when $p_{N_2} \approx 1$ atm no TiN can be formed at moderate temperatures (1200 K $< T <$ 1800 K) until TiO_2 has reduced to Ti_3O_5 or Ti_3O_5-based solutions, which agrees with the experimental results. It can therefore be assumed that the initial system has now transformed to a point where TiN formation from classical gas–solid reaction can take place. Similarly, modifying the externally applied p_{N_2} will affect the minimum degree of TiO_2 reduction (i.e. the n value) necessary for the first appearance of TiN.

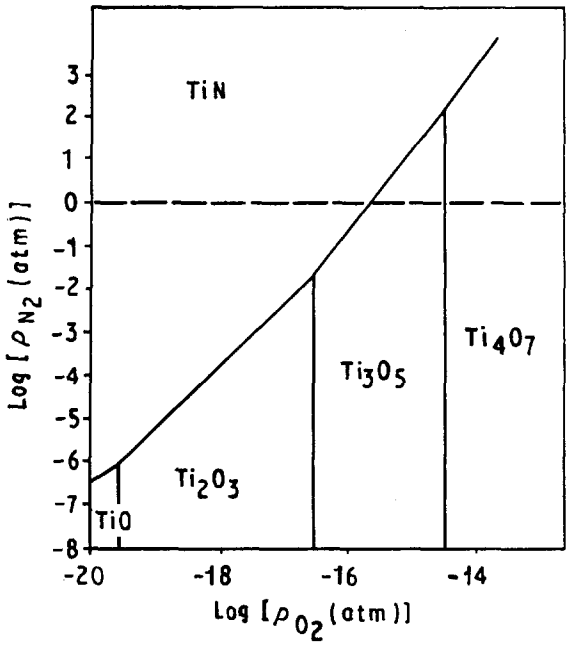

Figure 8 Calculated equilibrium phase diagram of Ti–O–N system at 1600 K.

3.3. Final reaction step: nitridation of mixed oxides

Major microstructure changes take place during the final stage of reaction (Figs 9 and 10). It is first to be noted that the titanium aluminium oxides become fractionated into a very fine porous particulate Al_2O_3 + TiN composite layer progressing toward the centre of the grains (Fig. 9). If it is assumed that the free energy of formation of $Al_xTi_yO_5$ is not very different from that of Ti_3O_5 or Ti_3O_5-based solutions, then according to available thermochemical information (Fig. 8) the nitridation of such phases by 1 atm N_2 appears feasible in the temperature range of interest here. The corresponding chemical reaction may be written as

$$Al_xTi_yO_5 + \frac{y}{2}N_2 \rightarrow \frac{x}{2}Al_2O_3 + yTiN + \frac{10-3x}{2}O_2 \quad (5)$$

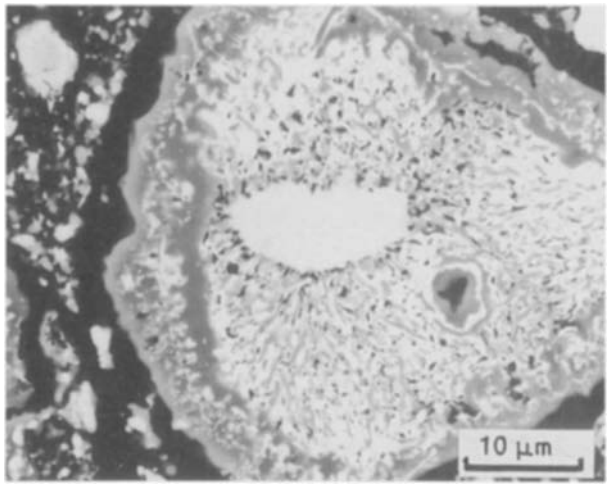

Figure 9 Microstructure of $Al_xTi_yO_5$ particle during its decomposition into Al_2O_3 + TiN.

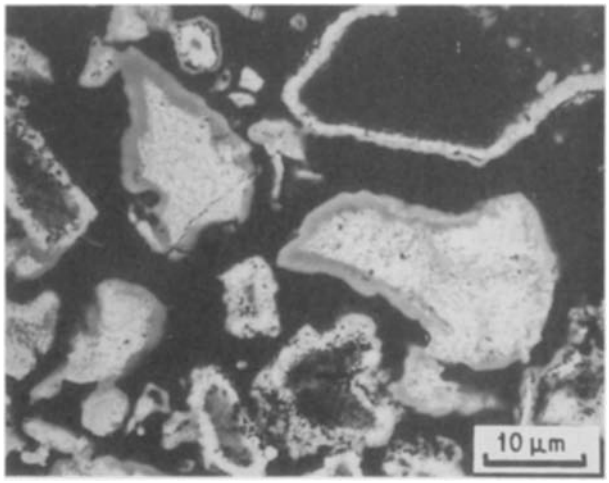

Figure 10 Final-stage microstructure of reacting coarse AlN + TiO_2 particle mixture. Composite Al_2O_3–TiN particles are covered with (grey) Al_2O_3 layers while hollow AlN particles are held by porous (white) TiN shells.

and it may be pointed out that the fine porosity which is also apparent on micrographs (Fig. 9) is likely to have resulted from the relative molar volume change associated with the above reaction, i.e. $\Delta V/V \approx -35\%$ for $\sim 3.82 \times 10^3\,kg\,m^{-3}$ specific gravity of aluminium titanate estimated from lattice parameter measurements at $x \approx 0.5$.

Further proof of $TiN + Al_2O_3$ formation was obtained as a result of heat-treating $Al_xTi_{3-x}O_5$ (pre-synthesized from $Al_2O_3 + 13TiO_2$, i.e. $x \sim 0.4$, in reducing conditions [18] at 1500 K in a 75% N_2 + 25% H_2 atmosphere. The TiN thus produced in the third reaction stage (labelled "secondary" to distinguish it from the "primary" TiN layers deposited on AlN) has the characteristic gold-yellow colour and measured lattice parameter $a_0 = 0.4240(3)$ nm, in good agreement with accepted standards [21]. Complementary local analyses using electron energy-loss spectroscopy (EELS) on a thinned sample in a Philips 430 electron microscope suggested [22] that residual oxygen concentrations do not exceed $\sim$ 1 wt %, i.e. $\sim$ 4 at %, in such TiN grains.

Finally, another typical feature of third reaction-stage microstructures is the development of continuous Al_2O_3 layers on the decompositing titanium suboxides (Figs 3d, 9 and 10). It is tempting to relate the growth of such layers to the formation of porosity which is also observed simultaneously in the as-yet unreacted AlN phase (Figs 3d and 10). The amounts and sizes of such pores may grow until the solid Al nitride has been essentially consumed, leaving thin hollow shells of primary TiN. It thus seems likely that some amounts of Al-containing vapour species were formed and transported via the gas phase to recondense as Al_2O_3 under conditions which will be further investigated. It can therefore be observed that the reaction promotes some redistribution within the initial TiO_2 particles of the Al_2O_3 produced, together with an important refinement of the particles as TiN.

4. Summary and conclusion

A detailed analysis of solid-phase evolution during the displacement reaction in $1.5TiO_2 + 2AlN$ powder mixtures has been performed. No external load was applied during heat treatments, so that only limited densification was recorded due to the generation of porosity by the chemical process itself. It was found that to a first approximation the chemical process may be broken down into three essential steps which are presented below for the simpler case of fine powders (FF samples) treated under a nitrogen pressure of one atmosphere.

Step 1:

$$\frac{3}{2}TiO_2 = \frac{3}{8}Ti_4O_7 + \frac{3}{16}O_2$$

$$2AlN + \frac{3}{16}O_2 = \frac{7}{4}AlN + \frac{1}{8}Al_2O_3 + \frac{1}{8}N_2$$

Step 2:

$$\frac{3}{8}Ti_4O_7 + \frac{1}{8}Al_2O_3 = \frac{3}{5}Al\frac{5}{12}Ti\frac{5}{2}O_5$$

$$\frac{3}{5}Al\frac{5}{12}Ti\frac{5}{2}O_5 + \frac{3}{4}N_2 = \frac{3}{2}TiN + \frac{1}{8}Al_2O_3 + \frac{21}{16}O_2$$

Step 3:

$$\frac{7}{4}AlN + \frac{21}{16}O_2 = \frac{7}{8}Al_2O_3 + \frac{3}{4}N_2 + \frac{1}{8}N_2\uparrow$$

Balance:

$$1.5\,TiO_2 + 2AlN = 1.5TiN + Al_2O_3 + \frac{1}{4}N_2$$

In such a description, reaction coupling is effected through adequate production and consumption of gaseous nitrogen and oxygen, respectively. It is also apparent that the most significant and complex changes occur in the initial TiO_2 phase. AlN is merely oxidized to Al_2O_3 in a continuous way during the whole process. The latter reaction has therefore been written with stoichiometric coefficients designed to somewhat artificially match the concurrent evolutions within the titanium phases.

Although roughly consistent with qualitative observations, such a scheme is either incomplete or even to be criticized in several respects. Although it involves two N_2 outgassing steps as already reported [12], the present analysis predicts identical 1.7 wt % outgassing at both the early and final stages of the overall reaction. This is somewhat different from the observed [12] 2.4% and 1.7% figures, respectively, and is thought to indicate that the coupling of the different reactions may be more complicated than proposed here or that other secondary reactions may take place such as the already-mentioned probable further $Al_xTi_yO_5$ enrichment in Al_2O_3 before the mixed oxide starts to nitride. On the other hand the proposed sets of equations only take into account two types of gas transport, namely O_2 and N_2, although microstructural evidence exists which indicates that both Ti and Al are also transported to a certain extent through the vapour phase. In the companion paper [16] attention will thus be paid to the composition of the reaction atmosphere in order to better describe the gaseous fluxes that may proceed during the conversion of $AlN–TiO_2$ to $TiN–Al_2O_3$.

Acknowledgements

Thanks are due to Mr G. Burri for the electron microprobe work, and to the Swiss National Science Foundation for financial support under Contract No. 0.4.842.0.85.19.

References

1. G. J. YUREK, R. A. RAPP and J. P. HIRTH, *Metall. Trans.* **4** (1973) 1293.

2. *Idem., ibid.* **10A** (1979) 1473.
3. C. TANGCHIVITTAYA, J. P. HIRTH and R. A. RAPP, *ibid.* **13A** (1982) 585.
4. J. A. van BEEK, P. de KOOK and J. J. van LOO, *Oxid. Met.* **22** (1984) 147.
5. J. J. van LOO, J. A. van BEEK, G. F. BASTIN and R. METSELAAR, *ibid.* **22** (1984) 161.
6. J. C. VORSTERS, J. Th. LAHEIJ, J. J. van LOO and R. METSELAAR, *ibid.* **20** (1983) 147.
7. R. ABRAMOVICI, *Mater. Sci. Engng* **71** (1985) 313.
8. E. Di RUPO and M. R. ANSEAU, *J. Mater. Sci.* **14** (1979) 705.
9. *Idem., ibid.* **14** (1979) 2924.
10. R. W. RICE, *Mater. Res. Soc. Symp. Proc.* **32** (1984) 358.
11. G. BAYER and A. MOCELLIN, *Rev. Chim. Min.* **23** (1986) 80.
12. A. MOCELLIN and G. BAYER, *J. Mater. Sci.* **20** (1985) 3697.
13. B. GROBÉTY, T. SPERISEN and A. MOCELLIN, *Sci. Ceram.* **14** (1987) 315.
14. B. GROBÉTY and A. MOCELLIN, *Ceram. Int.* **15** (1989) 271.
15. T. SPERISEN, P. MOECKLI and A. MOCELLIN, in Proceedings of International Conference on Powder Metallurgy PM '86, Düsseldorf, 1986 (Ausschuss F. Pulvermetall, P.O. Box 921, D-5800-Hagen) p. 1159.
16. T. SPERISEN and A. MOCELLIN, *J. Mater. Sci.* **27** (1992) 000.
17. B. FREUDENBERG and A. MOCELLIN, *J. Amer. Ceram. Soc.* **70** (1987) 33.
18. T. SPERISEN and A. MOCELLIN, *J. Mater. Sci. Lett.* **10** (1991) 831.
19. "JANAF Thermochemical Tables", 2nd Edn (National Bureau of Standards, 1971, Supplements 1974, 1975, 1982).
20. D. GOLDBERG, *Rev. Int. Hautes Temp. Réfr.* **5** (1968) 181.
21. A. CHRISTENSEN, *Acta Chem. Scand.* **A29** (1975) 563.
22. T. STOTO, Private Communication (1989).

Received 20 December 1990
and accepted 13 May 1991